



Simulation and Analysis the Attenuation Effect of Atmospheric Layers on a Laser Beam Within the Visible Range

Mohammed Kamal Saleh* 

Department of Physics, College of Education for Pure Sciences Ibn Al-Haitham, University of Baghdad, Baghdad, Iraq.

Thair Abdulkareem Khalil Al-Aish 

Department of Physics, College of Education for Pure Sciences Ibn Al-Haitham, University of Baghdad, Baghdad, Iraq.

*Corresponding Author: mohammed1985kamal@gmail.com

Article history: Received 31 October 2022, Accepted 21 November 2022, Published in July 2023.

doi.org/10.30526/36.3.3093

Abstract

The power and the size of the final spot of the laser beam reaching the target are very important requirements in most of the laser applications and fields such as medical, military, and scientific, so studying laser propagation in the atmosphere is a very important topic. The propagation of the laser beam through the atmosphere is subject to several attenuation processes that deplete the power and expand the beam. Through the simulation results of the free electron laser within the visible region of the electromagnetic spectrum (400-700nm), it was found that the attenuation increases with decreasing wavelength. Laser propagation in the presence of rain and snow leads to a very large loss of power compared to propagation in normal weather conditions free of rain and snow. Atmospheric turbulence depends largely on changes in temperature, so the turbulence decreases with altitude from sea level, which makes laser work at high altitudes, such as the stratosphere, a good option with better results.

Keywords: Free Electron Laser, Attenuation Coefficient, M^2 , Gaussian Beam, Atmospheric Turbulence

1. Introduction

In recent years, lasers have been used in many aspects of our lives, including communications, defense, industry, and scientific research. Studying the variables that influence the laser beam's power, beam diameter, and other characteristics is therefore crucial and necessary. The propagation of laser beams and the final spot size are important factors in most laser applications.



The propagation of laser beams in atmospheric layers is subject to attenuation operations (scattering, absorption, rain, snow, etc.) and atmospheric turbulence. The final power of the laser and beam divergence are affected by these phenomena [1,3]. The primary determinants of the performance quality of light effects are the features of the light source's beam and how they change along the optical axis of propagation and throughout the beam. The transverse mode (TEM00), which is similar to the output light for single-mode optical devices, defines the output of many laser devices built and used to produce or emit this mode (TEM00). The ideal (TEM00) beam is distinguished by the symmetry and revolution of the optical axis, in addition to having the maximum intensity in the center. Its intensity is consistent with that of the Gaussian beam [2].

In this study, laser beam propagation in the atmosphere will be examined, and the effects of attenuation operations on laser beams in the visible range (400–700 nm) will be calculated in terms of power loss and beam divergence.

2.Theory

In this study, the laser is obtained within the visible range through the free electron laser system (FEL). An FEL consists of three important components: (an electron accelerator, an undulator, and an optical resonator. FEL has important and unique features, as it can obtain a laser of any wavelength within the range from IR to X-rays. The following equations are used to calculate the required wavelength [4-5]:

$$\lambda = \frac{\lambda_w}{\gamma^2} \left(\frac{1}{2} + \frac{K^2}{4} \right) \quad (1)$$

$$K = \frac{e \lambda_w \beta_w}{2\pi m_e c} = 93.22 \times \lambda_w \times \beta_w \quad (2)$$

Where e : charge of electron, m_e : mass of electron, λ_w the undulator period length, γ the relativistic factor, β_w Intensity of magnetic field c : velocity of light and E_{beam} the energy of the beam. The magnetic field of an undulator B_w can be calculated by[6]:

$$B_w = 4.22 \exp \left[-\frac{g_w}{\lambda_w} \left(5.08 + 1.54 \frac{g_w}{\lambda_w} \right) \right] \quad (3)$$

Where g_w is the distance between the poles of the undulator.

The output power P_w from the undulator can be calculated by[6][7]:

$$P_w = P_{in} N \exp\left(\frac{L_w}{L_g}\right) \quad (4)$$

Where P_{in} is initial power, N the number of coherent photon per electron, L_w length of undulator and L_g the gain length

Finally, the following equation determines the total power of the free electron laser that emerges from the optical resonator[7],[9]:

$$P = P_w \exp(-\sigma d) \quad (5)$$

P : is the total power of laser, P_w is the output power from the undulator, σ is attenuation coefficient and d is the path length[10].

Note: Saturation power P_{sat} given in this relation $P_{sat} = \chi (E_{beam} \times I_{beam}) = 0.001(1250 \times 10^6 \times 10000) = 12.5Gw$. Where, χ is Pierce parameter and I_{beam} is the current of electron beam.

When the laser beam exits the aperture of the mirror and propagates in the atmosphere, it undergoes a deviation from the axis of propagation according to diffraction theory. As a result, depending on the atmosphere's density, length of the propagation axis, and interactions with components of the atmosphere, The final spot size of the laser changes due to wave propagation. In this paper, the propagation of a Gaussian TEM00 laser beam in the atmosphere within the visible spectrum (400–700 nm) will be investigated and simulated. The basic radius of a laser beam W_o can be calculated by[11]–[13]

$$W_o = \left[\frac{L \lambda}{\pi} \right]^{1/2} \quad (6)$$

The final radius of central Gaussian beam in Near-Mid Field given by[14] can be as follows:

$$W = W_o \left[\left[1 + \left(\frac{d \lambda}{\pi W_o^2} \right)^2 \right] \right]^{1/2} \quad (7)$$

In Far field, the final radius of laser beam is given by[11]:

$$W = W_o + \frac{d \lambda}{\pi W_o} \quad (8)$$

According to diffraction theory, as the propagation axis length increases, so does the diameter of the laser beam. The laser beam divergence can be calculated using the following equation[2], [10]:

$$\theta = \frac{M^2 \lambda}{\pi W_o} \quad (9)$$

The Rayleigh range is an important parameter in determining the propagation field of the laser beam in the near, mid, and far field, and the Rayleigh range value can be calculated using the following equation[2], [11]:

$$Z = \frac{\pi W_o^2}{\lambda} \quad (10)$$

The quality factor, which is the ratio between the theoretical Gaussian beam and the actual, is utilized to determine the performance quality of any optical device. The quality factor can be calculated by[11-12]:

$$M^2 = \frac{W}{W_o} \quad (11)$$

The atmosphere is composed of a variety of gases, some of which are present in varying amounts; the main gases are hydrogen, nitrogen, oxygen, and so on, which are drawn to the earth by gravity. The density of the atmosphere varies with altitude, temperature, and pressure. The atmosphere is divided into five layers based on pressure and temperature. Interactions with atmospheric particles and gases influence laser beam propagation in the atmosphere. Laser beam power is lost as a result of these interactions, and beam divergence occurs[15-16].

The propagation of laser beams through the atmosphere is a topic that has been of considerable theoretical and practical interest for a long time. When a laser beam propagates through the atmosphere, it subject to attenuation operations such as absorption, scattering, rainfall,

snowfall, and turbulence. The laser beam interacts with atmospheric components such as gases, particles, dust, smoke, and so on, and the amount of absorption and type of scattering depend on the relationship between the size of the atmospheric components and the wavelength of the laser beam. As a result of these interactions, the final laser power is reduced. The following equation is used to calculate the amount of absorption and scattering attenuation[9], [15]:

$$\sigma_{ab+sc} = \frac{3.912}{d} \left[\frac{550}{\lambda} \right]^q \quad (12)$$

Where, d altitude and λ laser wavelength in (nm).

Attenuation also occurs when it snows and rains. Since the size of the snowflake is larger than the raindrops, the loss in power of the laser transmitted during snowfall is more significant compared to the beam transmitted during rain. Thus, it represents a significant obstacle in the path of the laser beam. The amount of attenuation coefficient due to snowfall can be calculated by the equation[11-12]:

$$\sigma_{sn} = qS^u \quad (13)$$

Where S is the snow rate in millimeters per hour and (q, u) represents the value of dry and wet snow. The attenuation coefficient due to rainfall can be calculated by the following equation[11], [12]:

$$\sigma_{ra} = 1.076 S^{0.67} \quad (14)$$

The movement of air between the layers of the atmosphere and close to the Earth's surface causes large fluctuations in air density and refractive index, which result in turbulence in the air. These fluctuations are caused by the change in temperature and pressure with altitude. Atmospheric turbulence greatly affects the propagation of light waves. The amount and strength of atmospheric turbulence decrease with altitude above sea level. The refractive index is a function of temperature and pressure, and can be calculated by[11], [15]:

$$n = 1 + \left[\frac{77.6 \times 10^{-6} \times P}{T} \right] \left[1 + \frac{7530}{\lambda^2} \right] \quad (15)$$

λ is laser wavelength in (nm). The amount of turbulence can be calculated from the structural refractive index parameter C_n^2 with the following equation[11], [15], [17]:

$$C_n^2 = \langle (n_2 - n_1)^2 \rangle \times d^{-\frac{2}{3}} \quad (16)$$

Where, n_1 : the refractive index of first area, n_2 : the refractive index of second area and d the distance between two areas.

The Fried parameter is a crucial variable when examining how turbulence in the atmosphere affects the propagation of a Gaussian laser beam. It represents the circular diameter over the beam that preserves coherence in the propagation path length. Strong turbulence is indicated by the Fried parameter's highest value, and vice versa. The Fried parameter can be calculated by[11], [15][18]:

$$r_o = 0.33 \times \lambda^{\frac{6}{5}} \times \left(d^{\frac{3}{5}} \times C_n^2 \right)^{-\frac{3}{5}} \quad (17)$$

3. Results and Discussion

The results for this paper were obtained using Matlab software in version R2018b, where a program was developed to simulate the spread of a Gaussian beam from a free electron laser in the visible range. To generate a visible laser, a free electron laser was simulated using the designed implementation simulation program (400-700nm). A variety of factors, including the undulator

period, relativistic factor, static magnetic field, undulator gap, and others, have an effect on the laser's wavelength, according to the simulation. The table below depicts a portion of the simulation of a free electron laser for obtaining the required laser.

Table 1: Shows the simulation of Free Electron Laser.

E (PJ)	Relativistic γ	λ FEL (nm)	PFEL (GW)
40	487.864	760.822	312.928
42	512.258	690.086	345.003
44	536.651	628.777	378.645
46	561.044	575.29	413.847
48	585.437	528.348	450.619
50	609.83	486.926	488.95
52	634.224	450.189	528.85
54	658.617	417.46	570.314
56	683.01	388.174	613.342
58	707.403	361.865	657.933
60	731.797	338.142	657.933

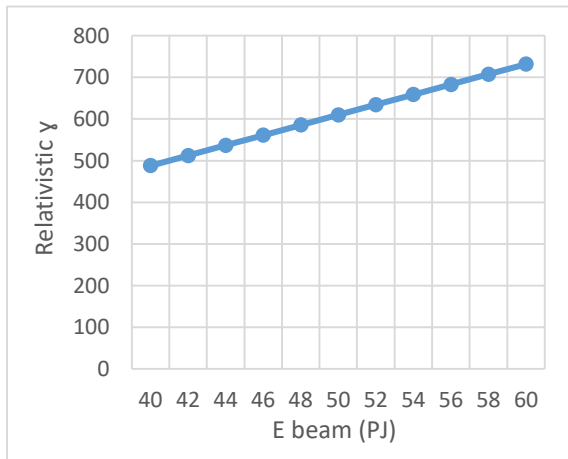


Figure 1. The relation between E beam and γ .

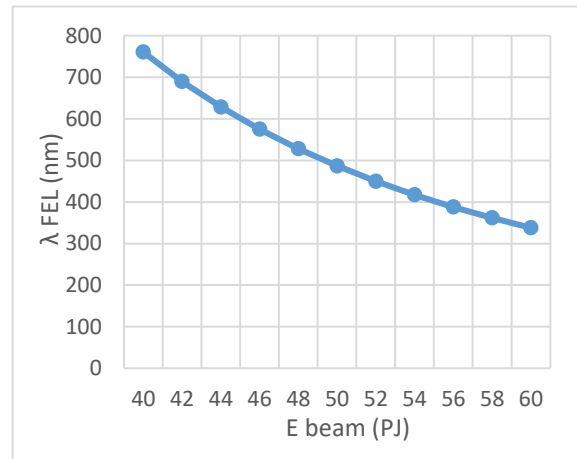


Figure 2. The relation between λ FEL and E beam.

The amount of electron beam energy that affects the wavelength of the free electron laser system is shown in **Table 1** and **Figures 1 and 2**. According to equation 1, the laser wavelength is inversely proportional to the relativistic factor. The relativistic factor increases as the energy of the electron beam increases, implying that the laser wavelength is inversely proportional to the energy of the electron beam.

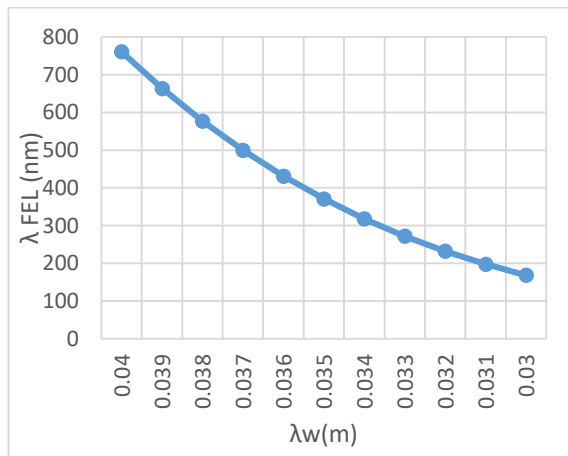


Figure 3. The relation between λ FEL and λw

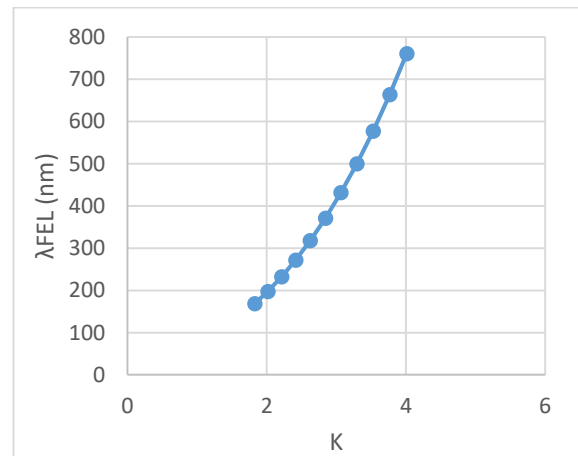


Figure 4. The relation between λ FEL and K.

The undulator period is the second factor in calculating the FEL. Figure 3 shows that the FEL increases as the undulator period increases and vice versa. Where the electron is accelerated and decelerated as it moves between the poles of the undulator. When it moves up and down, it emits energy in the form of a photon. According to Eq 1, reducing the undulator period results in a decrease in the wavelength FEL generated by the undulator as well as an increase in power. The undulator parameter is also an important factor in calculating the wavelength of the laser. The wavelength is directly proportional to the magnitude of the undulator parameter, i.e., the greater the value of the undulator parameter, the greater the wavelength, and vice versa. The other factor that affects the amount of laser wavelength is the undulator parameter, which is directly proportional to the wavelength according to Equation 1, where the higher the value of the undulator parameter, the greater the amount of wavelength generated from the free electron laser system and vice versa, as shown in **Figure 4**.

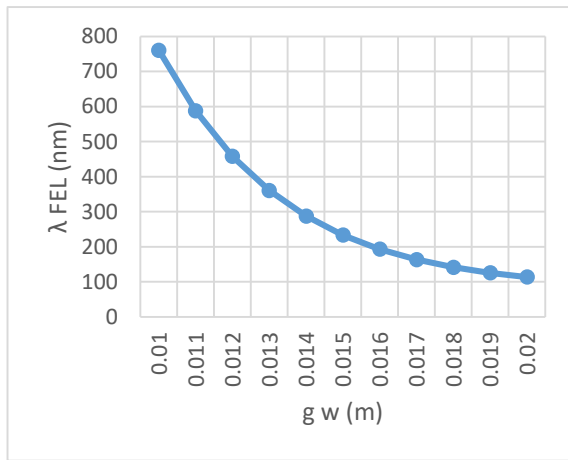


Figure 5. The relation between g w and λFEL

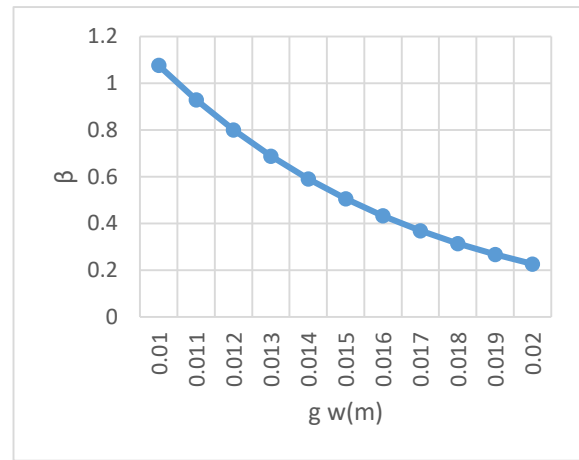


Figure 6. The relation between g w and β .

According to Equation 3, the strength of the static magnetic field (β) is proportional to the magnitude of the gap between the two poles, where the magnetic field strength decreases (i.e., inversely proportional) with an increase in the gap of the undulator, as shown in Figure 5, and since the value of the undulator parameter (K) is proportional to the strength of the static magnetic field (β) according to Equation 2, it turns out to behave similarly (i.e., inversely proportional). According to Eq. 1, the laser wavelength is proportional to the magnitude of the undulator gap; the wavelength decreases as the undulator gap decreases.

The propagation of the laser beam through the atmosphere is critical, and according to diffraction theory, the propagation laser beam will be subject to deviation in its path, resulting in beam expansion due to a variety of factors such as density, attenuation processes, and atmospheric turbulence. Eq. 8 calculates the radius of the laser beam produced by the mirror aperture. With a 10m optical resonator length and λ_{FEL} (690.086 nm), the basic radius of the laser is equal to 0.00148247 m, as illustrated in **Table 2**.

Table 2: shows the Gaussian beam propagation in altitude (1-11km).

λ nm	initial w_0 (m)	d (Km)	final w (m)	M2	Divergence
690.086	0.00148247	Mean sea level	0.00148247	1	0.000148248
690.086	0.00148247	1	0.14973	101	0.014973
690.086	0.00148247	2	0.297978	201	0.0297979
690.086	0.00148247	3	0.446225	301	0.0446227
690.086	0.00148247	4	0.594473	401	0.0594476
690.086	0.00148247	5	0.74272	501	0.0742723
690.086	0.00148247	6	0.890968	601	0.0890971
690.086	0.00148247	7	1.03922	701	0.103922
690.086	0.00148247	8	1.18746	801	0.118746
690.086	0.00148247	9	1.33571	901	0.133572
690.086	0.00148247	10	1.48396	1001	0.148397
690.086	0.00148247	11	1.63221	1101	0.163222

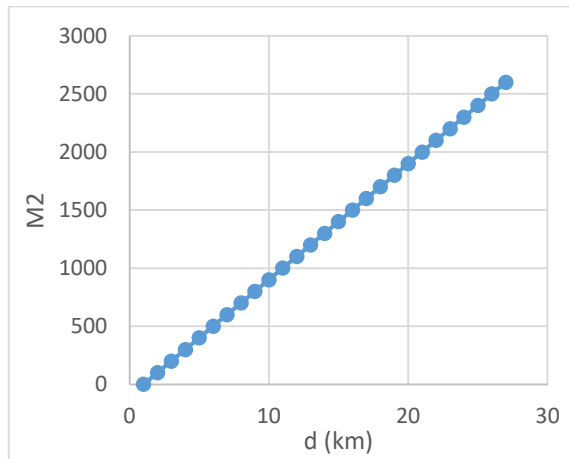


Figure 7. The relation between M2 and height d.

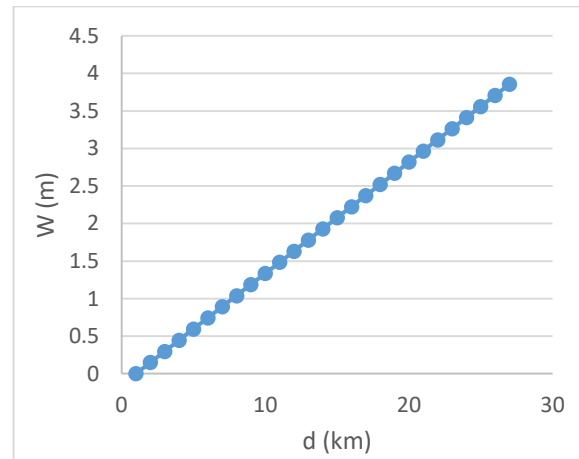


Figure 8. The relation between W (m) and height d.

Figures 7 and 8 show the divergence of the fundamental laser beam as well as the quality factor values of the laser beam traveling through the atmosphere, in accordance with Table 2. In this example, the expanded laser beam radius has deviated from the ideal value of the basic beam radius because it grows as the propagation path length (height) does. Additionally, because the quality factor depends on how much of the expanded radius is present, as determined by Eq. 13, its value has deviated from the ideal value. The value of the quality factor indicates ($M2=101$) an increase in the base laser beams radius at altitude ($d=1\text{km}$). The amount of quality factor present is determined by the extended beam radius, which is determined by the Rayleigh field. The greater the Rayleigh field, the greater the distance the beam can travel without deviating from the ideal value, and the less power is lost.

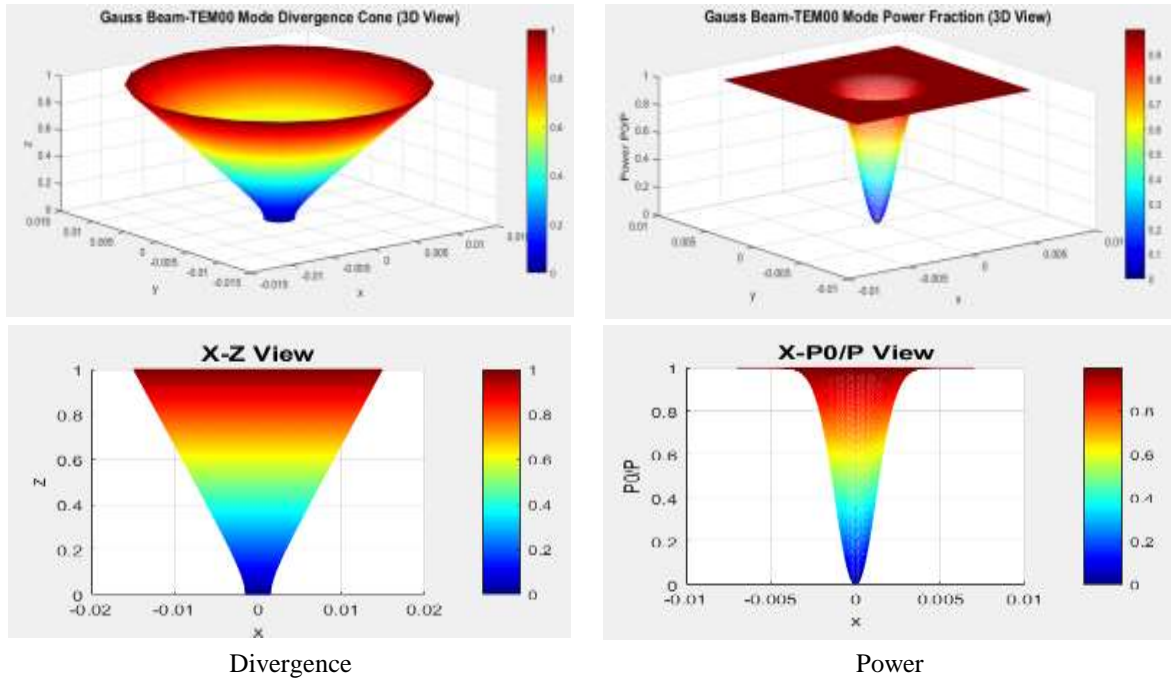


Figure 9. Shows The divergence and power of gaussian beam of FELin 2D and 3D.

Figure 9 depicts the divergence cone of the free electrode laser's Gaussian beam as well as the amount of power. The divergence grows with height, and the cone contains approximately 87% energy. To achieve high directional beams, short wavelengths with a large spot size must be used. As the wavelengths get longer, the divergence gets smaller. The power, on the other hand, is largely determined by the amount of frequency and the Rayleigh field, as it is directly proportional to the frequency and inversely proportional to the wavelength. When it comes to the Rayleigh field, it is highly dependent on the distance traveled, in the case of constant distance, as well as the amount of the Rayleigh field. **Figure 9** represents the divergence and power of a Gaussian beam with a frequency of (434241GHz) i.e. (690.086nm) in 2 and 3 dimensions.

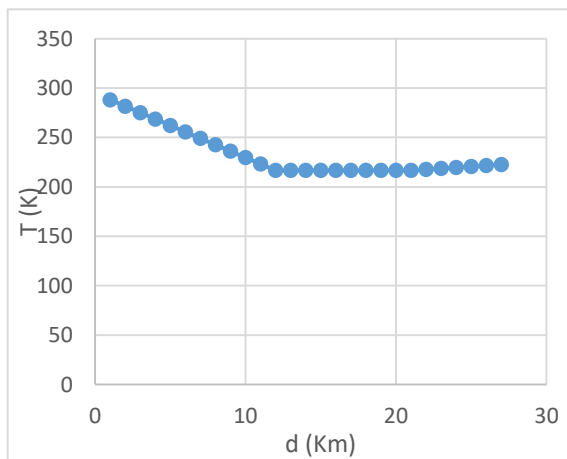


Figure 10. The relation between T and height d .

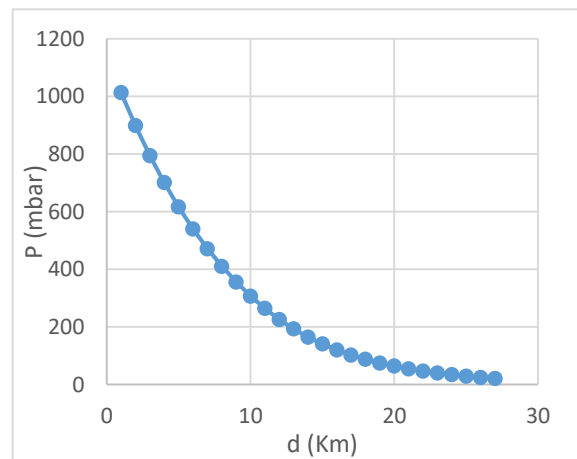


Figure 11. The relation between P and height d.

Figures (10 and 11) show the correlation between altitude above sea level and temperature and pressure. As the altitude increases above sea level, the temperature in the troposphere, the first layer of the atmosphere, will decrease by a fixed amount known as the decreasing constant, which equals 6.5 kelvin per kilometer (temperature is inversely proportional to altitude). The relationship is inverse because pressure decreases as altitude increases. As altitude above sea level rises, the atmospheric pressure decreases because a drop in temperature causes a drop in the kinetic energy

of the atmosphere's gaseous constituents. As you ascend above sea level, density will behave similarly because it is influenced by temperature and pressure.

Table 3. The attenuation coefficient of various visible wavelength with intial power (1000MW)

d (km)	$\lambda = 690.086 \text{ nm}$		$\lambda = 528.348 \text{ nm}$		$\lambda = 417.46 \text{ nm}$	
	$\sigma(\text{sc+ab})$ (1/km)	power (MW)	$\sigma(\text{sc+ab})$ (1/km)	final P (MW)	$\sigma(\text{sc+ab})$ (1/km)	final P (MW)
1	3.42573	32.5255	4.005	18.2243	4.59675	10.0846
2	1.6548	36.5308	2.01476	17.7829	2.39675	8.28341
3	1.07681	39.5405	1.34894	17.4779	1.64554	7.17882
4	0.792199	42.0542	1.01516	17.238	1.26339	6.38656
5	0.623526	44.2619	0.814474	17.037	1.0309	5.77337
6	0.51227	46.2534	0.680439	16.863	0.874057	5.27729
7	0.4161	54.3288	0.588811	16.2173	0.799784	3.70346
8	0.364088	54.3286	0.51521	16.2172	0.699811	3.70346
9	0.323634	54.3285	0.457964	16.2173	0.622055	3.70343
10	0.29127	54.3288	0.412168	16.2172	0.559849	3.70345
11	0.264791	54.3288	0.374698	16.2173	0.508954	3.70344

Table 3 displays the attenuation coefficients for three wavelengths of visible light (the study area) due to absorption and scattering. It is evident that the attenuation coefficient increases as the laser wavelength decreases (inverse proportion), according to equation 12. Furthermore, it is evident from **Table 3** that the amount of loss power of a laser varies depending on the laser wavelength, which is related to the amount of attenuation. It has been observed that the final power will decrease with each of the three wavelengths as they get shorter.

Table 4. The final power after attenuation for laser beam

d (Km)	q	Without Snow & Rain Attenuation		With Snow & Rain Attenuation	
		$\sigma(\text{Sc+ab})$ (1/km)	final P (MW)	$\sigma \text{ tot}(1/\text{km})$	Final P (W)
1	0.585	3.42573	32.5255	6.213433	2002360
2	0.737	1.6548	36.5308	4.442503	138450
3	0.8437	1.07681	39.5405	3.864513	9225.58
4	0.9287	0.792199	42.0542	3.579902	603.283
5	1.00034	0.623526	44.2619	3.411229	39.2231
6	1.063	0.51227	46.2534	3.299973	2.51795
7	1.3	0.4161	54.3288	3.203803	0.182075
8	1.3	0.364088	54.3286	3.151791	0.0112088
9	1.3	0.323634	54.3285	3.111337	0.000690017
10	1.3	0.29127	54.3288	3.078973	0.00004248
11	1.3	0.264791	54.3288	3.052494	0.000002615

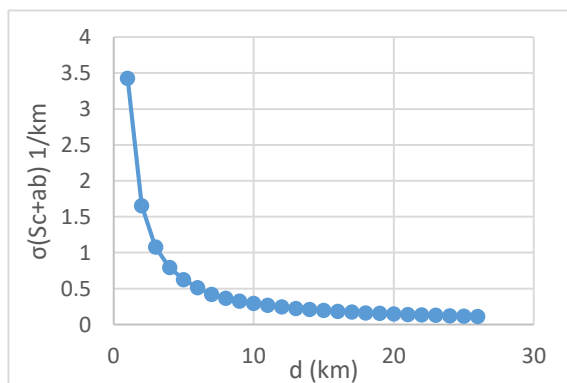


Figure 12. The relation between (σ) and altitude d Without Snow & Rain Attenuation

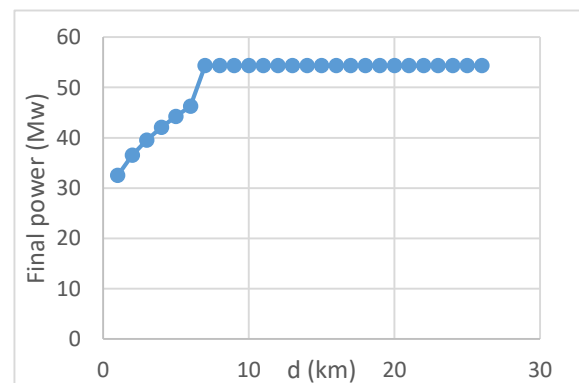


Figure 13. The relation between power and d (km) Without Snow & Rain Attenuation

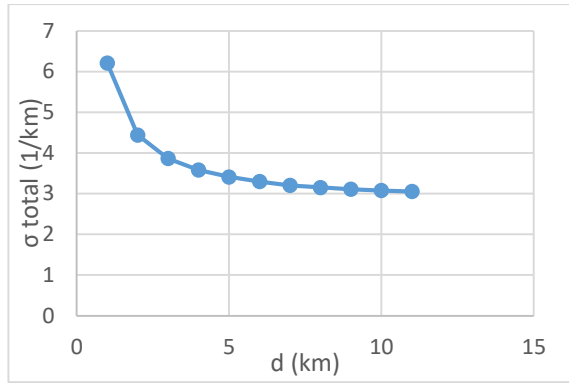


Figure 14. The relation between (σ) and altitude d With Snow & Rain Attenuation.

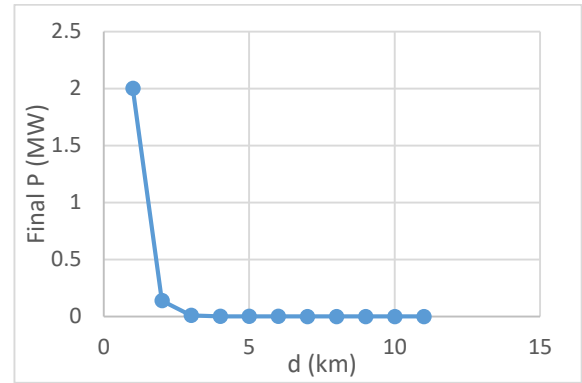


Figure 15. The relation between power and d (km) With Snow & Rain Attenuation.

Table 4 and Figures (12-15) show the magnitude of the loss power of the laser beam ($\lambda_{FEL} = 690.086nm$ and $P_o = 1000MW$) with and without snow and rain attenuation. From Figures 12 and 13, we see that the amount of loss in the final laser power that reaches the target depends largely on the amount of the attenuation coefficient, which in turn depends on the wavelength of the laser beam. As we explained earlier and in Figures 13 and 14, we see that the amount of loss due to attenuation without adding rain and snow attenuation will gradually decreases with increasing altitude, as the greatest loss is in the first 1 km due to the high density and abundance of particles, such as dust grains, dust, etc., that increase the amount of attenuation. At a height of 8 km or more, the attenuation coefficient begins to stabilize at very close values, as in Figures 14 and 15. The attenuation coefficient and power loss with the presence of rain and snow attenuation show that the amount of power coming out of the device, which is 1000 MW, has greatly diminished with altitude. This is due to the fact that the attenuation of snow is greater than the attenuation of rain, which in turn is greater than the attenuation of absorption and scattering because the size of the snowflake is very large and causes a large attenuation of the laser power.

Table 5. Show the change of main parameters of atmosphere turbulence with altitude

d (km)	Temp K	P mbar	n	Cn2 (m -2/3)×10 ⁻¹²	ΓO (m)
1	281.65	898.661	1.000251513	5.670571469	0.006209001
2	275.15	794.801	1.0002277	4.861187818	0.006810082
3	268.65	700.883	1.000205652	4.15180548	0.0074861
4	262.15	616.162	1.000185276	3.532029414	0.008248656
5	255.65	539.933	1.000166483	2.99263363	0.009110992
6	249.15	471.527	1.000149183	2.524397765	0.010090278
7	242.65	410.317	1.000133295	2.120009731	0.011204567
8	236.15	355.706	1.000118735	1.771712976	0.012478483
9	229.65	307.137	1.000105424	1.473187291	0.013939366
10	223.15	264.084	1.000093287	1.218339357	0.015622007
11	216.65	226.055	1.000082249	1.438072696	0.014142601
12	216.65	193.096	1.000070257	1.04925766	0.017087106
13	216.65	164.943	1.000060014	0.765580238	0.020644453
14	216.65	140.895	1.000051264	0.55867665	0.024940289
15	216.65	120.352	1.000043789	0.407604096	0.030133854
16	216.65	102.805	1.000037405	0.297417499	0.036406413
17	216.65	87.8162	1.000031951	0.217015223	0.043984907
18	216.65	75.0127	1.000027293	0.158348272	0.05314101
19	216.65	64.0759	1.000023314	0.115539666	0.064203564
20	216.65	54.7337	1.000019915	0.088903992	0.075135476
21	217.65	46.7536	1.000016933	0.064259327	0.09129271
22	218.65	39.937	1.000014398	0.046449308	0.110920099
23	219.65	34.1142	1.000012243	0.033575819	0.134766464
24	220.65	29.1404	1.00001041	0.024271411	0.163734722
25	221.65	24.8918	1.000008852	0.017555733	0.198859533

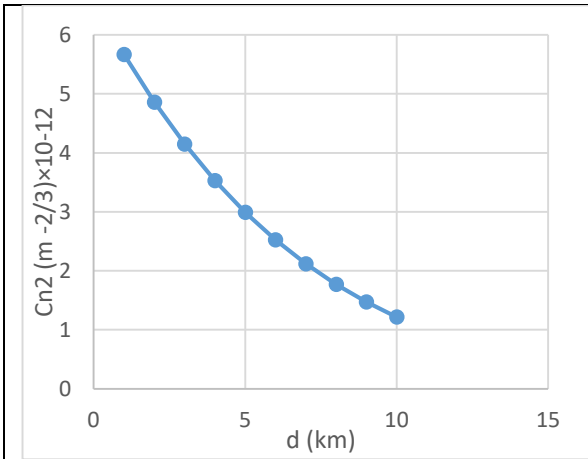


Figure 16. The relation between C_n^2 and d (km) in troposphere

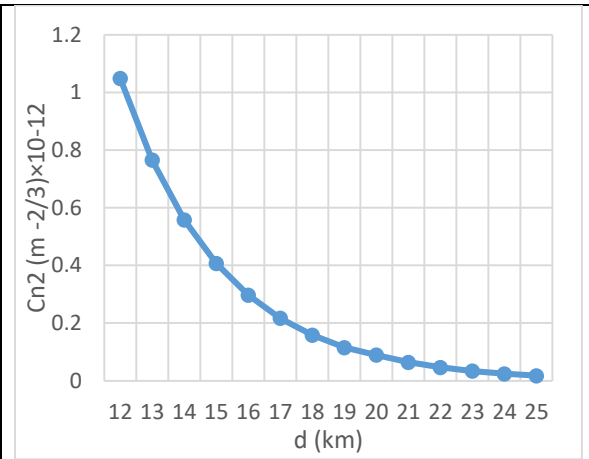


Figure 17. The relation between C_n^2 and d (km) above troposphere

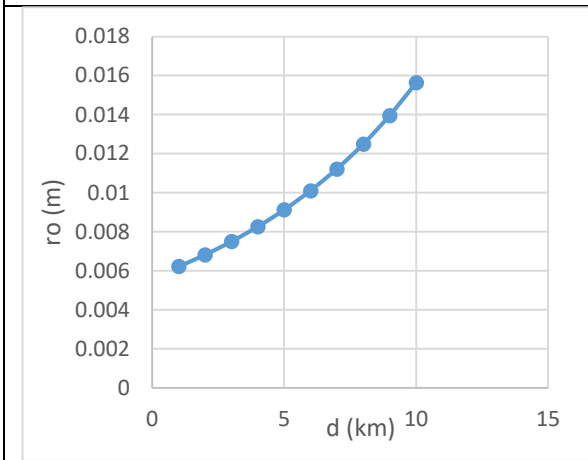


Figure 18. The relation between r_o (m) and d (km) in troposphere

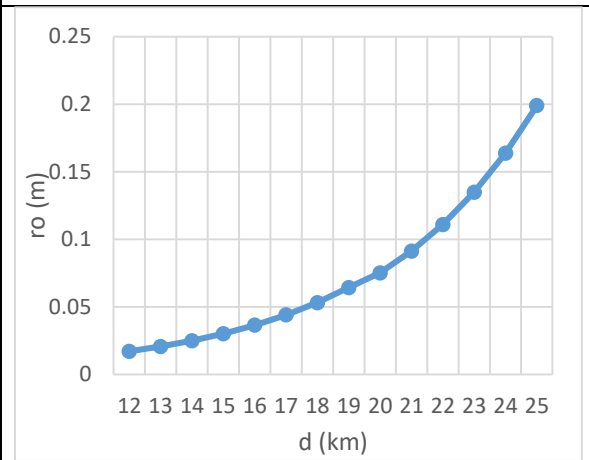


Figure 19. The relation between r_o (m) and d (km) above troposphere

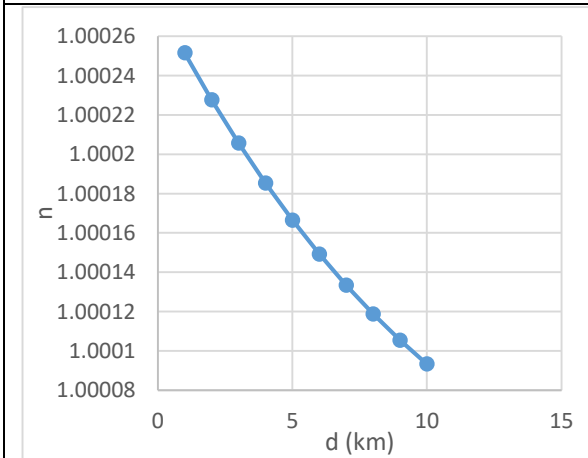


Figure 20. The relation between n and d (km) in troposphere

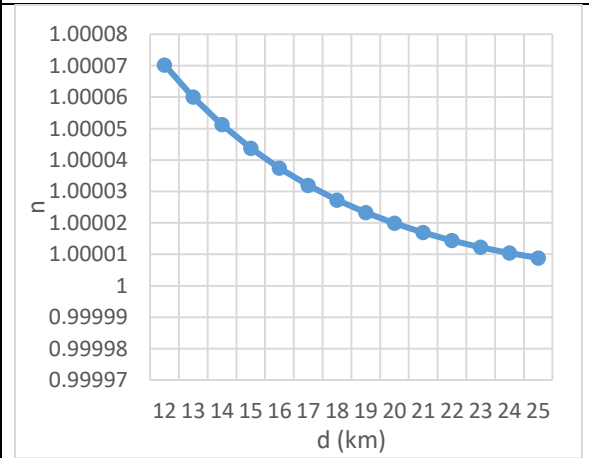


Figure 21. The relation between n and d (km) above troposphere

Table 5 shows the main parameters that go into calculating atmospheric turbulence. **Figures 16 and 17** show that the value of the structural refractive index C_n^2 decreases with increasing altitude from sea level due to the decrease in temperature with altitude, where fluctuations in temperature are a major cause of turbulence, as shown in equation 16. **Figures 18 and 19** show the values of a Fried parameter that increases with height inversely proportional to the structural refractive index, as shown in equation 17. The amount of air refractive index depends

largely on the amount of temperature, and therefore the refractive index will decrease with increasing height, which is linearly proportional to the temperature according to Equation 15. As shown in **Figures 20 and 21**, the structural refractive index is linearly proportional to pressure. From the above, it proves to us that temperature is the main factor in everything that occurs during turbulence in the atmosphere.

4. Conclusions

Through the simulation results in this study, we conclude that the laser can be produced in the free electron laser system at any desired wavelength by changing and manipulating the basic factors involved in calculating the wavelength, such as the energy of the beam, the undulator period, the undulator gap, etc. Also, the attenuation coefficient increases with short wavelengths, so, blue light is more susceptible to attenuation compared to red light. The greatest amount of absorption is near the surface of the earth due to the high density of air as well as the presence of particles and suspended objects such as dust, which increases the attenuation and thus the increase in the loss in the final power. The amount of atmospheric turbulence depends largely on the temperature fluctuation, so the atmosphere is more turbulent near the sea surface, and this turbulence decreases with an increase in altitude. The radius of the laser beam increases with the increase in height, which leads to an increase in the beam divergence.

References

1. Carlos, B.; Gómez, G.; Poliak, I. J.; Laser Beam Shaping, *Master's Thesis, Brno University of Technology*, **2012**.
2. de Prado, R. P.; García-Galán, S.; Muñoz-Expósito, J. E.; Marchewka, A.; Computer-aided laser-fiber output beam 3d spatial and angular design, *Symmetry*, **2020**, *12*, 1. doi: 10.3390/sym12010083.
3. Fahey, T.; Islam, M.; Gardi, A.; Sabatini, R.; Laser Beam Atmospheric Propagation Modelling for Aerospace LIDAR Applications, *Atmosphere (Basel)*, **2021**, *12*, 7, 918, doi: 10.3390/atmos12070918.
4. Lateef, R. T.; AL-Aish, T.; Design and Simulate a New Defense System of Free Electron Laser DSFEL, *Eng. Technol. J.* **2017**, *53*, 2, 166–172.
5. Al-Aish, T. A. K.; Jawad, R. L.; Kamil, H. A.; Design and simulation a high-energy free electron laser HEFEL, in *AIP Conference Proceedings*, **2019**, *2123*, 020068. doi: 10.1063/1.5116995.
6. Mahmood H. K.; Al-Aish, T. A. K.; Design and stimulated the detectors of high-power lasers DHPL, in *AIP Conference Proceedings*, **2020**, *2307*, 020025. doi: 10.1063/5.0032989.
7. Dhedan, Z. A.; Al-Aish, T. A. K.; Kamil, H. A.; Design and simulation of a new system for producing laser beams without resonator 'NSPLBR, in *AIP Conference Proceedings*, **2022**, *2437*, 1, 20012.
8. Ali, M. A.; Al-Aish, T. A. K.; Kamil, H. A.; A simulation breakdown the blood clot using a free electron laser system, in *AIP Conference Proceedings*, **2022**, *2437*, 1, 20021.

9. Al-Aish, T. A. K.; Kamil, H. A.; Simulation and Analysis the Effect of the Lorentz Force in a Free Electron Laser, *Ibn AL-Haitham J. Pure Appl. Sci.*, **2022**, 35, 2, 7–16,
10. Kamil, H. A.; Ahmed, M. S.; Al-Aish, T. A. K.; Rain formation by free electron laser pulse system FELPS, in *AIP Conference Proceedings*, **2019**, 2190, 020084. doi: 10.1063/1.5138570.
11. Jawad, R. L.; Calculating and Analysing of Some Atmospheric Effects on the Beam of Free Electron Laser, *Master Thesis ,University of Baghdad , Iraq*, **2017**.
12. AL-BASSAM, H. A. K.; Theoretical Study for the Design of a Free electron Laser System to Produce Artificial Rain in Iraq, *Master Thesis ,University of Baghdad, Iraq*, **2020**.
13. Alda, J.; Laser and Gaussian Beam Propagation and Transformation, in *Encyclopedia of Optical and Photonic Engineering, Second Edition*, Taylor & Francis, **2019**, 34, 1–15. doi: 10.1081/e-oe2-120009751.
14. Al-aish, T. A. K.; Design and Analysis the Fiber Laser Weapon System FLWS, *Adv. Phys. Theor. Appl.*, **2015**, 47, 59–69.
15. Al-Aish, T. A. K.; Analysis and study of the effect of atmospheric turbulence on laser weapon in Iraq, *Baghdad Sci. J.*, **2017**, 14, 2, 427–436, doi: 10.21123/ bsj.2017. 14.2.0427.
16. Kulikov, V. A.; Vorontsov, M. A.; Analysis of the joint impact of atmospheric turbulence and refractivity on laser beam propagation, *Opt. Express*,. **2017**, 25, 23, 28524,. doi: 10.1364/OE.25.028524.
17. Xu, M.; Shao, S.; Liu, Q.; Sun, G.; Han, Y.; Weng, N.; Optical Turbulence Profile Forecasting and Verification in the Offshore Atmospheric Boundary Layer, *Appl. Sci.*, **2021**, 11, 18, 8523, doi: 10.3390/app11188523.
18. Shao, S.; Qin, F.; Xu, M.; Liu, Q.; Han, Y.; Xu, Z.; Temporal and spatial variation of refractive index structure coefficient over South China sea, *Results Eng.* **2021**, 9, 100191, doi: 10.1016/j.rineng.2020.100191.